GlueX-doc-1795

The BCAL SiPM Array Readout

Fernando J. Barbosa

Jefferson Lab

8 August 2011

1. Introduction

The BCAL readout employs Hamamatsu 16-cell SiPM photo-detectors arranged in a 4 x 4 array. Each cell has 3600 pixels (50 μm x 50 μm) all connected in parallel (S12045). The 16 cells on an array are further connected in parallel for readout via a single preamp.

There are 3840 SiPM arrays with their preamp outputs summed in groups of 3 or 4. Each sum is then split and fed into a buffer (BCAL_A) and a gain of 10 amplifier (BCAL_T). BCAL_A will be readout via flash ADCs; BCAL_T will be readout via discriminators and TDCs (fig. 1).

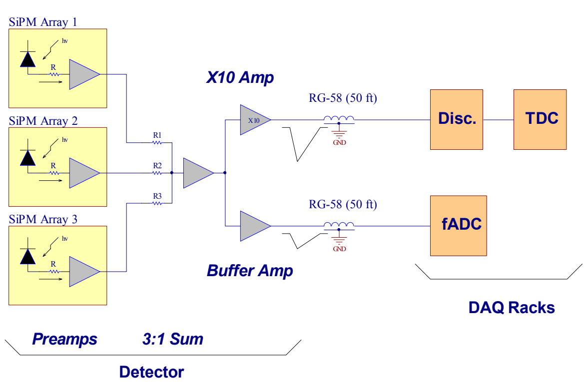

Fig. 1 – BCAL Readout Architecture

2. The SiPM

Electrical models and characterization of SiPMs have been previously reported [1], [2]. Fig. 2 shows the model for the BCAL SiPM.

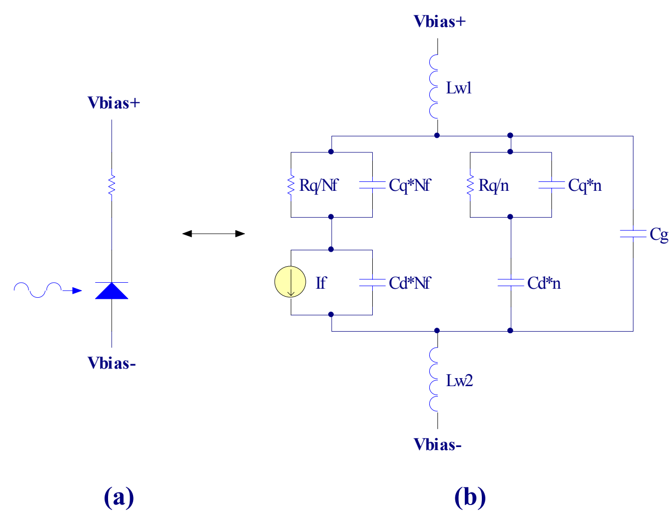

Fig. 2 – SiPM Model

A generic symbol for this type of photo-detector is shown on the left (a); its detailed electrical schematic is shown on the right (b). Typical model parameters are as follows:

Cd - Pixel capacitance (90 fF)
Cq - Quench stray capacitance (3 fF)
Rq - Quench resistor (150 kΩ)

Cg – Parasitic capacitance (50 pF)
Lw1,2 – Inductance of wire bond (1 nH)
Nf – Number of fired cells
n – Total number of pixels minus Nf.

Note that Lw1 is shared by 4 cells, which are connected together on the die, while Lw2 applies to each cell. *If* represents a current source for each fired pixel.

Prior to any excitation, the pixel capacitances (Cd) are all equally charged as a result of the applied bias (Vbias). Once a pixel fires as a result of a single photon being detected, Geiger multiplication causes a large current to discharge the respective pixel capacitance by a discrete amount of charge which, in turn, lowers the voltage across the reverse-biased diode, due to the quench resistor (Rq), and below a level sufficient to sustain multiplication. The pixel capacitance is then recharged via Rq with a recovery time constant $\tau \approx 20$ ns.

Geiger multiplication at the silicon level is very fast, of the order of 100 ps. However, the signal risetime (i.e., leading edge) depends on Cd, Cq, the equivalent diode forward impedance during discharge, inductances in the signal path and the temporal behavior of the pixels.

3. The BCAL Readout

The readout electronics is segregated from the SiPM arrays because of the need for thermal stability and cooling of the sensors. Fig. 3 shows a prototype section of the desired implementation under test.

The U-board will be affixed to the cooling plate and has the sockets for the electrical connections to the SiPM. Because the minimum distance between the cooling plate and the preamp/sum board is slightly less than 5 cm, the commercially available ultra-miniature (U.FL) bias and signal coaxial cables (5 cm long) are appropriate for this application.

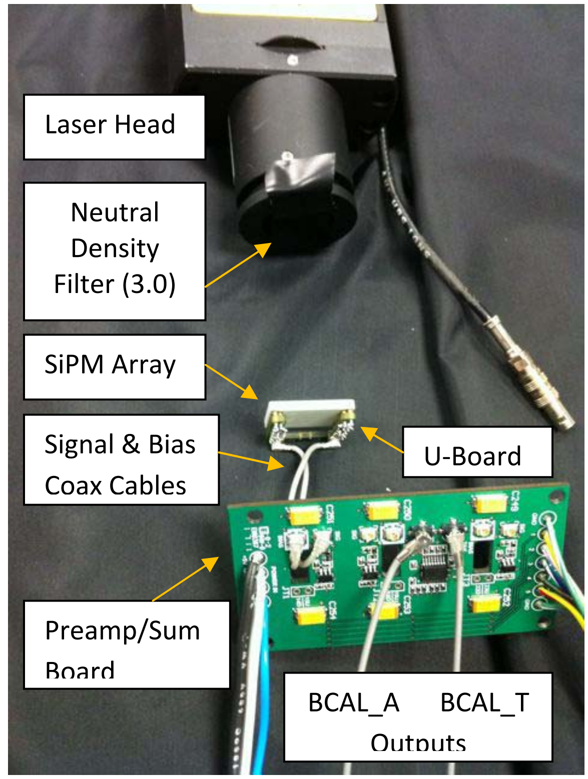

Fig. 3 – Prototype of BCAL Readout

The prototype Preamp/Sum board implements the functions shown in fig. 1 and has provisions for the bias temperature compensation. The output cables are commercially available miniature coaxial cables (H.FL).

4. Preamp/Sum Response

The Preamp/Sum impulse response was characterized by applying a short pulse with a very fast rise time of 460 ps. Fig 4 shows that the BCAL_T (purple) and BCAL_A (green) outputs behave very well.

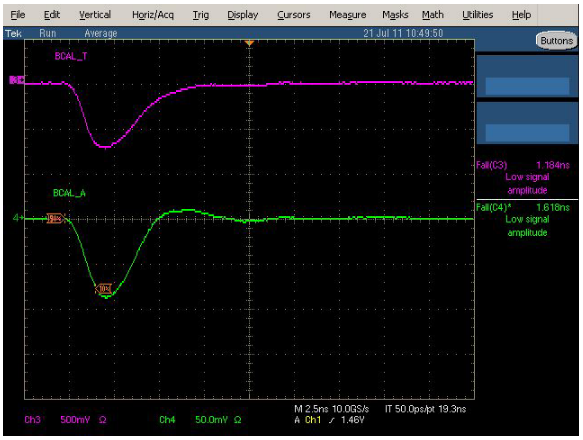

Fig. 4 – Preamp/Sum Impulse Response

The amplitudes scales reflect the gain ratio of a factor of 10 between the two outputs; the horizontal scale is 2.5 ns per division. The pulse widths are less than 3 ns and the rise times are less than 1.2 ns (note that the top pointer on the BCAL_A trace is incorrect and not at the 90% level). Unfolding the input risetime, the intrinsic risetime of the Preamp/Sum is **Tr = 1.1 ns**. This is in good agreement with simulation results.

5. BCAL Readout Characteristics

The intrinsic characteristics of the BCAL readout were obtained by using the Hamamatsu PLP-10 with a 405 nm laser head (fig. 3). The pulse width is rated at 70 ps at a wavelength of 405 nm; the output optical power and repetition rate are adjustable. A neutral density filter with a factor of 1000 attenuation was placed at the output of the laser. The Sync output from the laser controller was used to trigger the scope and serve as the reference for these measurements. The jitter of the Sync signal relative to the optical pulse is not specified by the manufacturer, however.

5.1 Readout Optimization

Fig. 5 shows a simplified schematic of the physical implementation of the U-board and interconnects to the preamp/sum board.

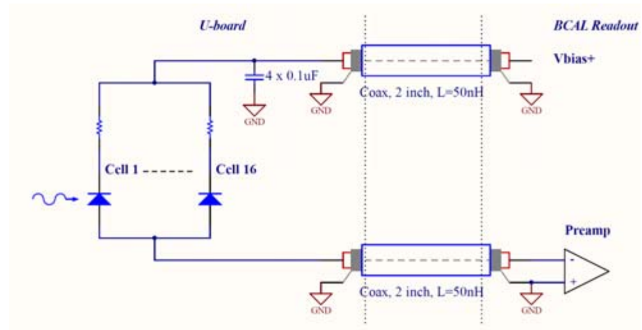

Fig. 5 – Schematic of Implementation

The inductances of the coaxial cables present multiple challenges to the signal integrity of the readout. On the signal side, the cable inductance limits the bandwidth over all frequencies of interest, thus increasing the signal rise time. The cable capacitance is much lower than the sensor capacitance and can be neglected. Increasing impedance in the signal path also increases the pulse width but this effect may not be significant due to the long recovery time of the SiPM.

Large currents are required to replenish the charge in the pixel capacitances during and just after Geiger multiplications, as mentioned above. Because this is of the order of 100 ps, the inductance of the coaxial cable feeding the bias to the SiPM array presents a very high impedance to the bias supply feed from the preamp/sum board.

The four 0.1 uF bypass capacitors on the U-board are of critical importance. They supply current to the SiPMs during short periods of high current demand preventing supply sag and, as importantly, provide a low impedance path for the signal return current from the preamp input stage.

The SiPM array can be simply modeled as a current source in parallel with the total sensor capacitance (**C**) of 5.1 nF. The sensor is then coupled to the preamp via the cable inductance (**L**) of 50 nH in series with the interconnection resistance plus the input impedance of the preamp (**r**). The resulting transfer function is:

$$H(s) = \frac{\left(\frac{1}{LC}\right)}{s^2+\left(\frac{r}{L}\right)s+\left(\frac{1}{LC}\right)} \qquad (1)$$

The time domain characteristics of this resonant circuit can be changed by adjusting the location of the two poles. It is possible to adjust the poles by adding a small series resistor with the input of the preamp. The variable **r** in (1) can then be replaced with **R**. The fastest risetime can be obtained when the poles coincide, i.e. the circuit is critically damped:

$$R = 2\sqrt{L/C} \qquad (2)$$

For the values noted above, R = 6.3 Ohm. In practice, R will increase the pulse width and it needs to be determined experimentally by considering the optical pulse characteristics for acceptable pulse widths and because of the preamp input impedance and interconnect resistances. The overall response characteristic of the readout consists of the convolution of the input optical pulses, the SiPM response, the interconnections and the preamp response at the desired gain.

Fig. 6 shows the response of the SiPM array with the optimized BCAL readout by adding a small equivalent series resistor of 2 Ohm.

Fig. 6 – Optimized BCAL Response

The signal labeled L-Trig (yellow) is the laser Sync output. Considering the BCAL-A, its risetime is 4.93 ns and its pulse width is 60 ns, as indicated by the vertical cursors. The BCAL_T has a slightly longer risetime of 6.23 ns and at a peak amplitude of about 1V.

Fig. 7 shows the response of the optimized BCAL readout together with the SiPM array signal probed at the U-Board with a wideband FET probe.

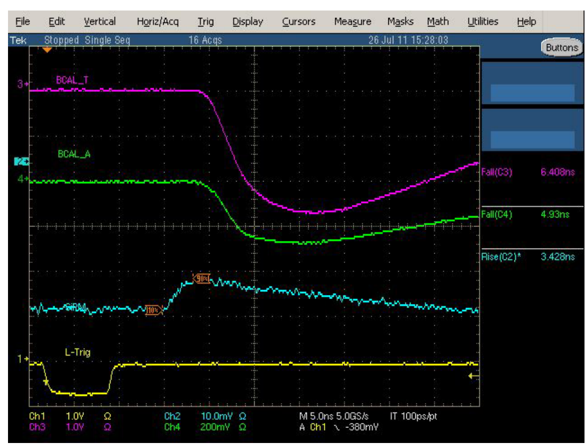

Fig. 7 – SiPM & BCAL Response

The SiPM array signal (light blue) has a risetime of 3.43 ns and the BCAL_A signal has a risetime of 4.93 ns.

5.3 Noise

Fig. 8 shows the peak-to-peak and rms noise measurements for the BCAL readout.

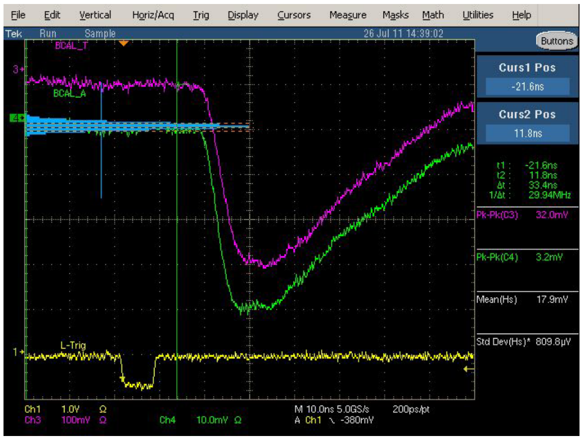

Fig. 8 – Noise Measurements

Noise on the BCAL-A output is 3.2 mVp-p or 0.8 mVrms, from the histogram. These are also in good agreement with simulations. Noise on the BCAL_T output is 32 mVp-p due to the factor of 10 higher gain. Considering the maximum BCAL_A output signal amplitude of 2.7V, a dynamic range in excess of 1600 can be expected.

5.5 Timing Resolution

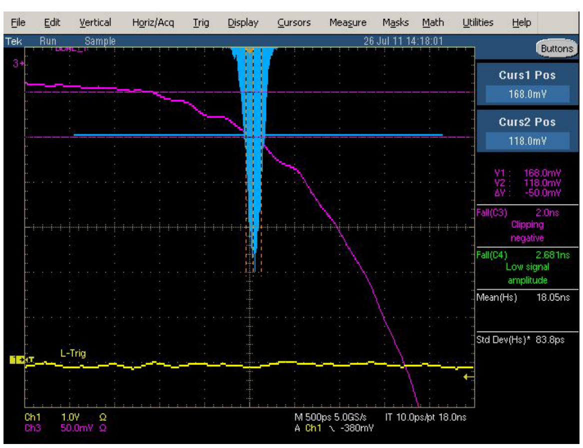

Fig. 9 – Timing Resolution Measurements

Fig. 9 shows the histogram of the time jitter (light blue) on the BCAL_T output. The signal amplitude on the BCAL_A was set at 175 mV or 6.5% of the dynamic range and the measurement level, or threshold, on the BCAL_T was set at 50 mV, as indicated by the horizontal cursors. The timing jitter histogram has an rms of 83.8 ps. This includes all contributions. As mentioned before, the time jitter for the laser pulse relative to the Sync output is not specified by Hamamatsu but it should be low. In such case, this measurement may well be representative of the timing resolution of the array as configured for the BCAL readout.

6. Preamp on Array Measurements

Additional tests were performed to determine the impact of relocating the preamp to the back of the SiPM array. Fig. 10 shows the arrangement as was previously developed.

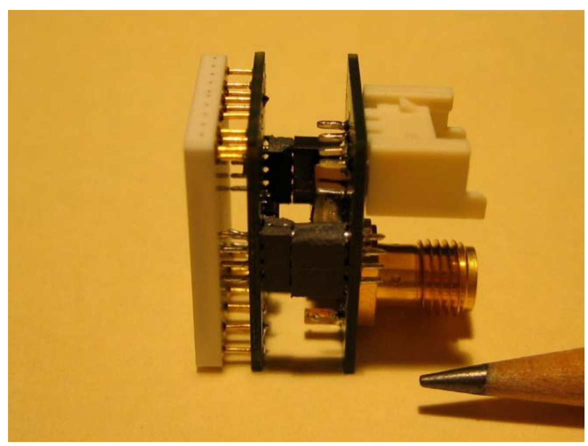

Fig. 10 – Preamp on Array Setup

The SiPM array is mounted on the same PCB as the preamp. The preamp was implemented exactly as on the BCAL Preamp/Sum readout but with an equivalent series resistor of 1 Ohm. The layout of the PCB is obviously different from the U-board.

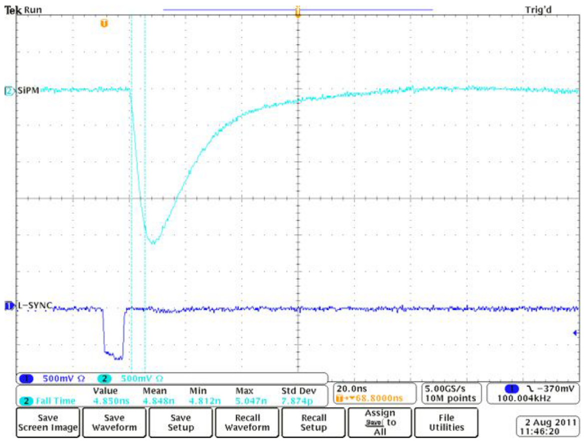

Fig. 11 – Preamp on Array Measurements

The risetime of the pulse is shown to be 4.85 ns and the pulse width (10%-10%) was measured to be 58 ns. These results are in very good agreement with the results obtained from the optimized BCAL readout.

7. Tests with an LED Source

Tests were also performed with a pulse generator and a blue LED to evaluate the behavior of the SiPM array and readout with optical pulses of different pulse widths.

Fig. 12 shows the results of circuit simulations from various pulse widths using the SiPM array model described above.

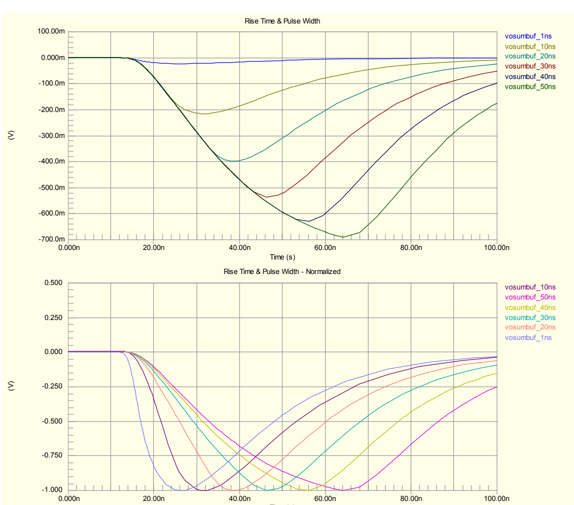

Fig. 12 – Simulations with Various Pulse Widths

The top panel shows that the pulse amplitudes and risetimes increase in proportion to wider input pulses, resulting from integration of the signal currents by the large SiPM array capacitance. The bottom panel shows the same waveforms after normalization: risetimes range from 5.4 ns to 33.4 ns for input pulse widths ranging from 1ns to 50 ns, respectively.

Figs. 13 and 14 show the response of the array to signal pulse widths of 5 ns and 40 ns, respectively, applied to the LED. The top traces labeled SiPM (light blue) are the array output pulses; the bottom traces labeled L-SYNC (dark blue) are replicas of the LED input pulses.

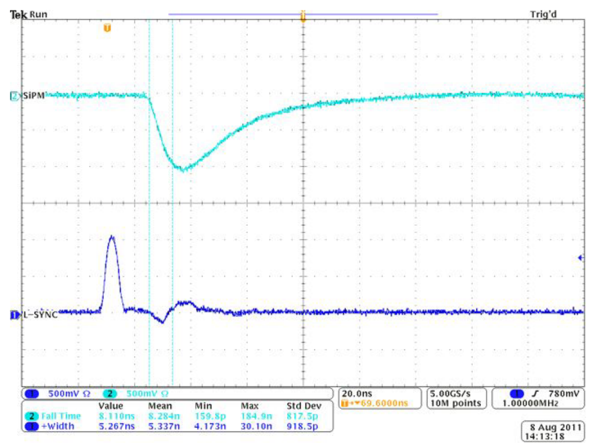

Fig. 13 – 5 ns LED Pulse – Tr=8.1 ns

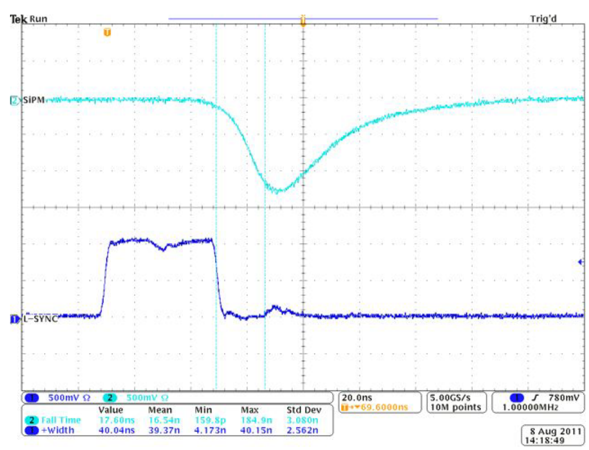

Fig. 14 – 40 ns LED Pulse – Tr=17.6 ns

The actual output pulse risetimes from the array are shorter than predicted from the simulations shown in fig. 12, a result of lower sensor capacitance at higher frequencies. Fig 15 shows a collection of superimposed output pulses from the array in response to LED input pulses of different widths. This should be compared to the top panel in fig. 12.

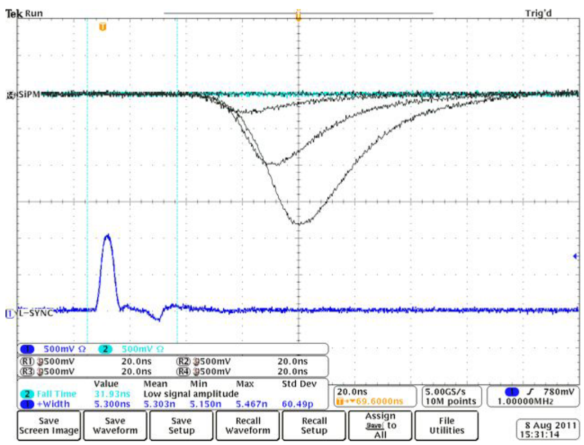

Fig. 15 – LED, Various Pulse Widths

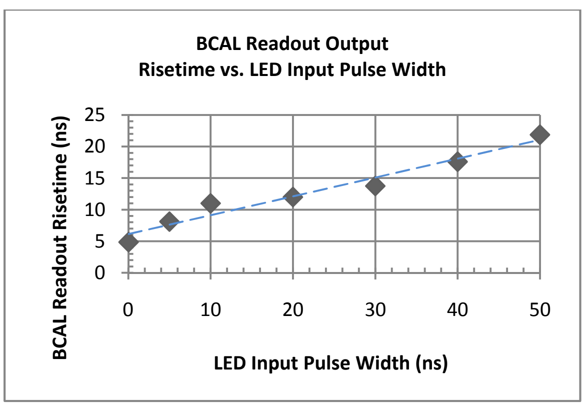

Fig. 16 – Rise Times and Pulse Widths

The plot in fig. 16 shows the risetime dependence of the BCAL readout on the input optical pulse width. A linear fit is shown by the dashed line. The intrinsic risetime of the readout, obtained with the laser, of 4.85 ns is included.

8. Conclusion

The BCAL Preamp/Sum readout electronics has been optimized with the SiPM array mounted on the U-board and connected to the Preamp/Sum board by ultra-miniature coaxial cables.

The BCAL readout has a fast preamp and sum with an intrinsic risetime of 1.1 ns, excellent noise performance of 3.2 mVp-p (0.8 mVrms), including the SiPM array, with a dynamic range capability in excess of 1600 and a pulse width of 60 ns. These numbers compare well with the stated requirements of a risetime less than 15 ns, a pulse width of less than 80 ns and a dynamic range of about 400.

The intrinsic risetime of the BCAL readout has been measured to be 4.85 ns by means of a very short laser pulse. The risetime and amplitude, or effective gain, were also determined to be dependent on the pulse width of the optical source. The BCAL detector employs scintillating fibers with fast characteristics and the resulting readout output pulse characteristics should be similar to those obtained with the laser.

Tests are currently underway to determine the timing resolution in more detail. Further tests will be performed for the expected photon dynamic range (88 to 36,000 photons) in order to scale the gain to fit within the fADC250 range. These tests should employ the final scintillating fiber configuration of the BCAL.

References

[1] H. T. van Dam et al, "A Comprehensive Model of the Response of Silicon Photomultipliers", *IEEE Trans. Nuc. Sci., vol.. 57, no. 4, pp. 2254-2266, Aug. 2010*.

[2] S. Seifert et al, "Simulation of Silicon Photomultiplier Signals", *IEEE Trans. Nuc. Sci., vol.. 56, no. 6, pp. 3726-3733, Dec. 2009*.